SUPPLEMENTAL MATERIALS

TLR4-dependent signaling drives extracellular catabolism of low-density lipoprotein aggregates

Rajesh K. Singh*[1], Abigail S. Haka*[1], Arky Asmal[1], Valéria C. Barbosa-Lorenzi[1], Inna Grosheva[1], Harvey F. Chin[1], Yuquan Xiong[2#], Timothy Hla[2] and Frederick R. Maxfield[1,#]

*These authors contributed equally to this work

[1]Department of Biochemistry, Weill Cornell Medical College, New York, NY 10065, USA
[2]Vascular Biology Program, Boston Children's Hospital and Department of Surgery, Harvard Medical School, Boston, MA 02115, USA
[#]Current address: Thoracic Service, Department of Surgery, Memorial Sloan Kettering Cancer Center, New York, NY 10065, USA

Running title: TLR4 regulates aggregated LDL catabolism

[#]To whom correspondence should be addressed: Dr. Frederick R. Maxfield, Department of Biochemistry, Box 63, Weill Cornell Medical College, 1300 York Avenue, New York, NY 10065, USA. E-mail: frmaxfie@med.cornell.edu. Tel: +1 646 962 2759; Fax: 646 962 0519

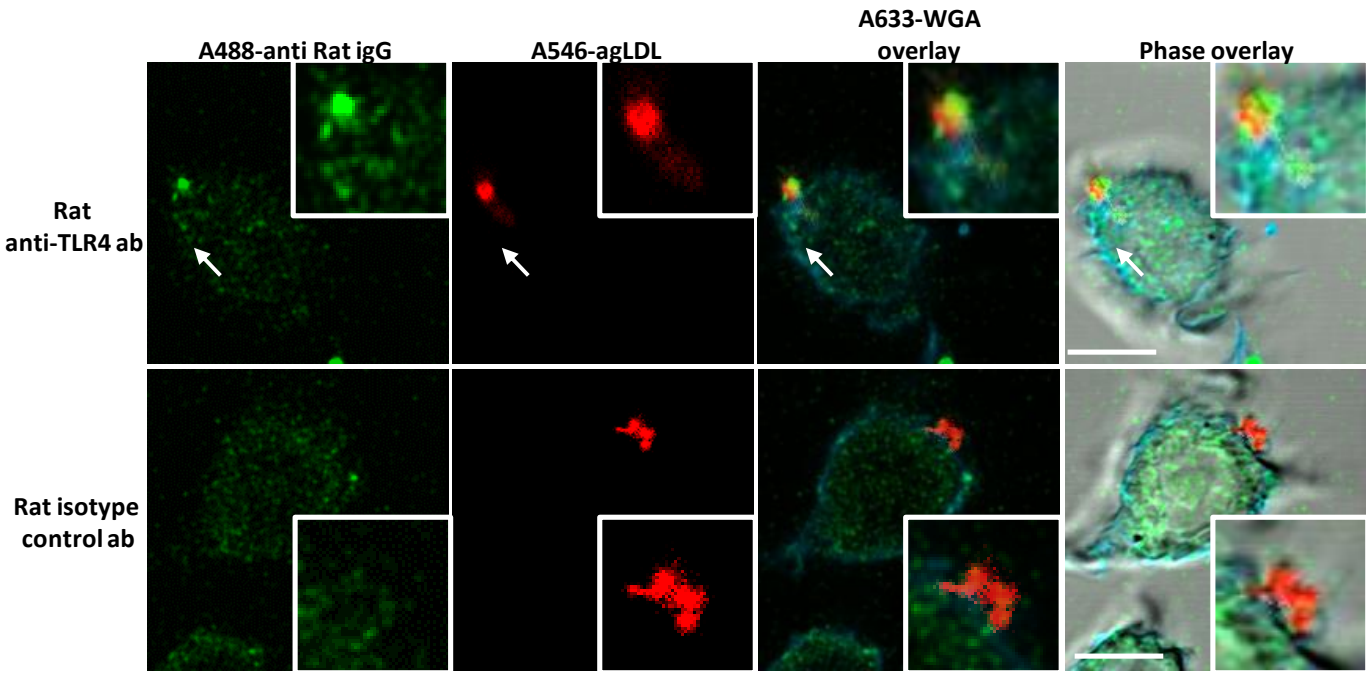

Figure I. TLR4 clusters in the vicinity of the LS. RAW264.7 macrophages were treated with A546-AgLDL for 1 hr and fixed using 3% PFA/0.5% glutaraldehyde. TLR4 was detected using a Rat anti-TLR4 antibody, followed by A488-anti Rat secondary antibody. Rat isotype control antibody was used to assess non-specific antibody binding. Cell plasma membrane was stained using A633-WGA. Arrow shows TLR4 clustering at the LS. Scale bars 20 μm.

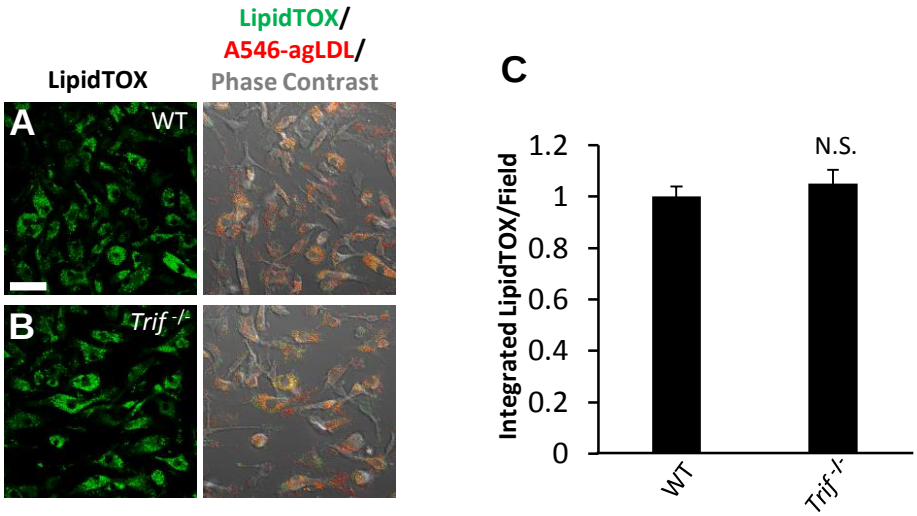

Figure II. TRIF does not regulate foam cell formation in response to agLDL. (A-B) Foam cell formation in response to agLDL was analyzed by confocal microscopy of (A) WT, (B) *Trif*$^{-/-}$ BMMs treated with A546-agLDL for 12 hr, fixed and neutral lipids stained using LipidTOX green. (C) Confocal images were used to quantify LipidTOX intensity per field. Data were compiled from 3 independent experiments per condition. Error bars represent the standard error of the mean (SEM). N.s. not statistically significant. Scale bar 40 μm.

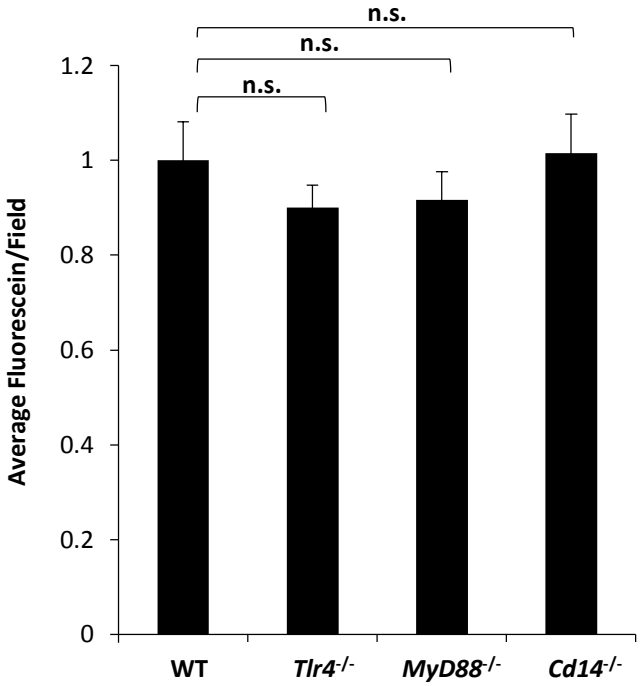

Figure III. Biotin-fluorescein-dextran loading control. No difference was seen in the pinocytosis of biotin-fluroescein-dextran between WT, *Tlr4*$^{-/-}$, *Myd88*$^{-/-}$ and *Cd14*$^{-/-}$ macrophages. Data were compiled from at least 3 independent experiments per condition. Error bars represent the SEM. n.s. is non significant.

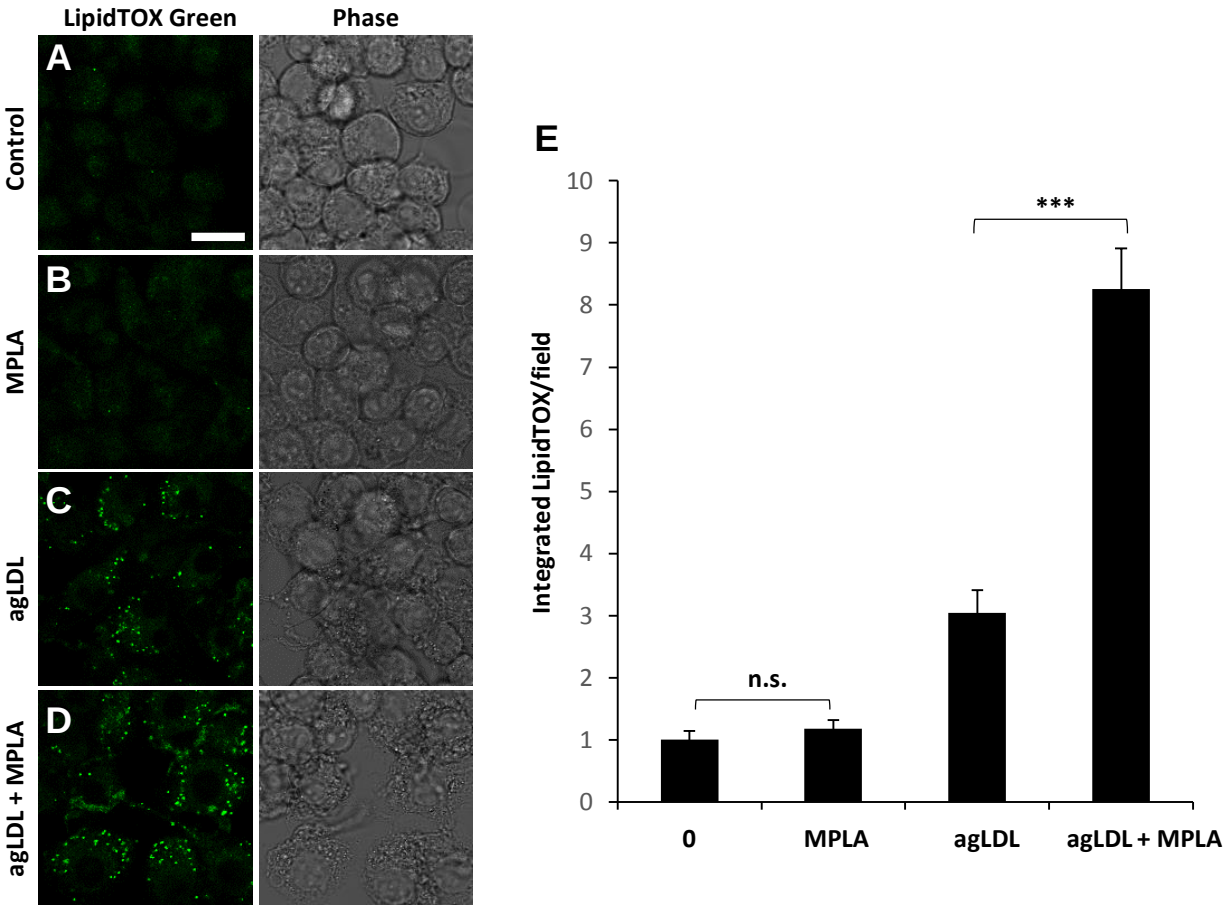

Figure IV. TLR4 activation by MPLA enhances foam cell formation in response to agLDL treatment. (A-D) J774 cells were left untreated (A, C) or pre-treated with MPLA for 1 hr (B, D) prior to agLDL treatment for 4 hrs (C-D). Cells were fixed using 3% PFA and neutral lipids stained using LipidTOX Green. Cells were analyzed by confocal microscopy. **(E)** Confocal images were used to quantify LipidTOX staining per field. Data were compiled from at least 3 independent experiments per condition. Error bars represent the SEM. *** $p \leq 0.001$. N.s. Not statistically significant. Scale bar 20 μm.

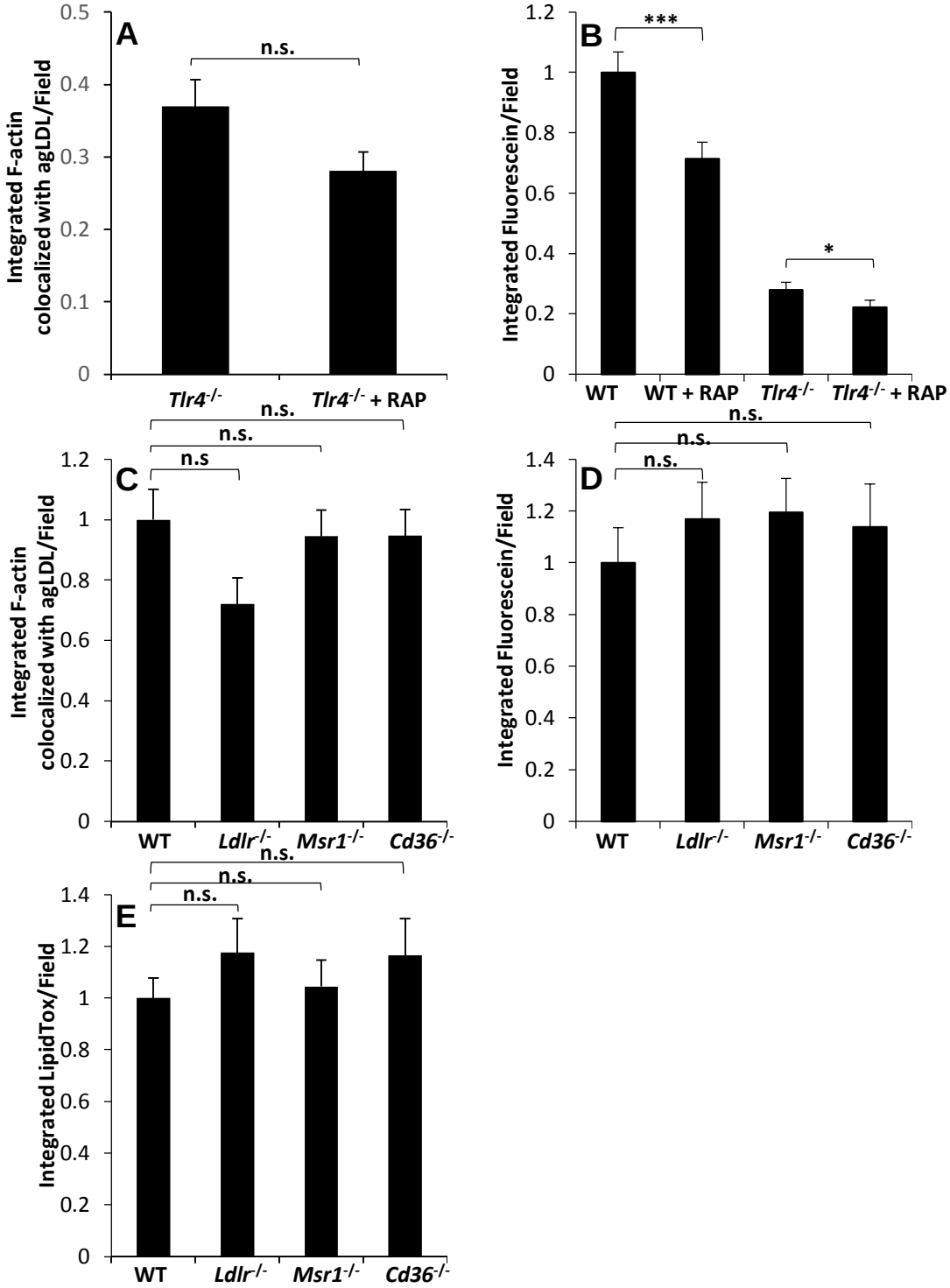

Figure V. LRP can promote lysosome exocytosis but LDLr, MSR1 and CD36 are not involved in actin polymerization, lysosome exocytosis and foam cell formation in response to agLDL. (A) *Tlr4*$^{-/-}$ BMMs were left untreated or pre-treated with RAP for 1 hr prior to incubation with A546-agLDL for 1 hr in the presence of RAP. Local F-actin rich structures used to form the compartment were quantified via confocal microscopy of A488-phalloidin stained samples and normalized to WT BMMs in the same experiments. (B) WT and *Tlr4*$^{-/-}$ BMMs with their lysosomes loaded with biotin-fluorescein-dextran were left untreated or pre-treated with RAP for 1 hr prior to incubation with streptavidin-A546-agLDL for 90 min in the presence of RAP. Exocytosis of biotin-fluorescein-dextran to aggregate containing compartments was quantified via confocal microscopy. (C) Quantification of the local F-actin rich structures used to form the lysosomal synapse in WT, *Ldlr*$^{-/-}$, *Msr1*$^{-/-}$ and *Cd36*$^{-/-}$ BMMs. (D) Quantification of lysosome exocytosis to aggregate containing compartments in WT, *Ldlr*$^{-/-}$, *Msr1*$^{-/-}$ and *Cd36*$^{-/-}$ BMMs. (E) Quantification of foam cell formation in WT, *Ldlr*$^{-/-}$, *Msr1*$^{-/-}$ and *Cd36*$^{-/-}$ BMMs incubated with A546-agLDL for 12 hrs, fixed and stained with LipidTOX green. Data were compiled from at least 3 independent experiments per condition. Error bars represent the SEM. * $p \leq 0.05$, *** $p \leq 0.001$. N.s. Not statistically significant.

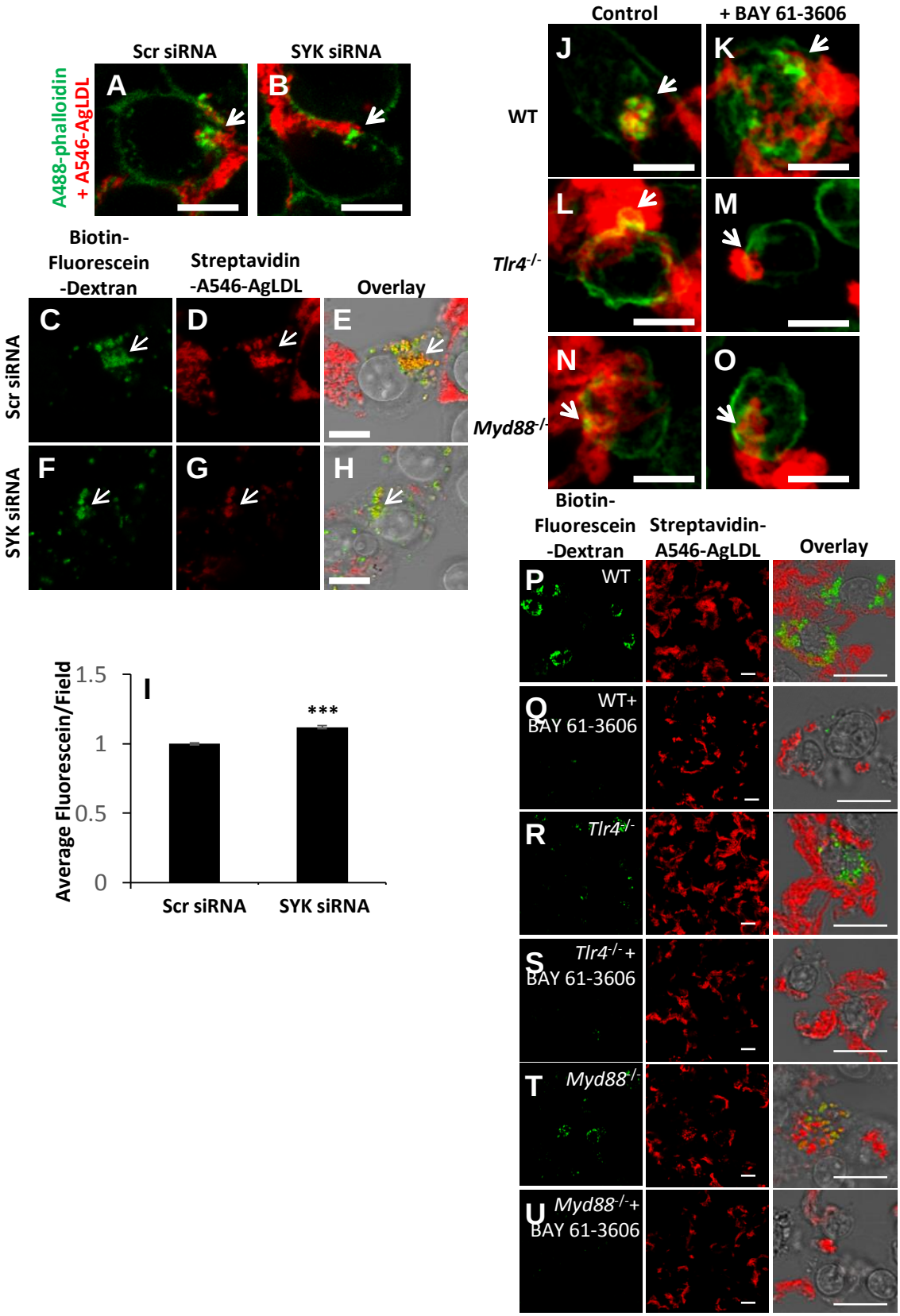

Figure VI. SYK can promote actin polymerization and lysosome exocytosis in response to agLDL. (A-B) Representative images from Figure 3C showing actin polymerization at the LS in Scr siRNA or SYK siRNA transfected J774 cells. (C-H) Representative images from Figure 3D showing lysosome exocytosis at the LS in Scr siRNA or SYK siRNA transfected J774 cells. (I) Scr siRNA or SYK siRNA transfected J774 cells were treated overnight with fluorescein-biotin-dextran and dextran loading in lysosomes was quantified via confocal microscopy. (J-O) Representative images from Figure 3E showing actin polymerization at the LS in WT, *Tlr4-/-* or *MyD88-/-* BMMs with or without BAY 61-3606 treatment to inhibit SYK. (P-U) Representative images from Figure 3F showing lysosome exocytosis at the LS in WT, *Tlr4-/-* or *MyD88-/-* BMMs with or without BAY 61-3606 treatment to inhibit SYK. Scale bars 20 μm. Data were compiled from 3 independent experiments. Error bars represent the SEM. *** $p \leq 0.001$.

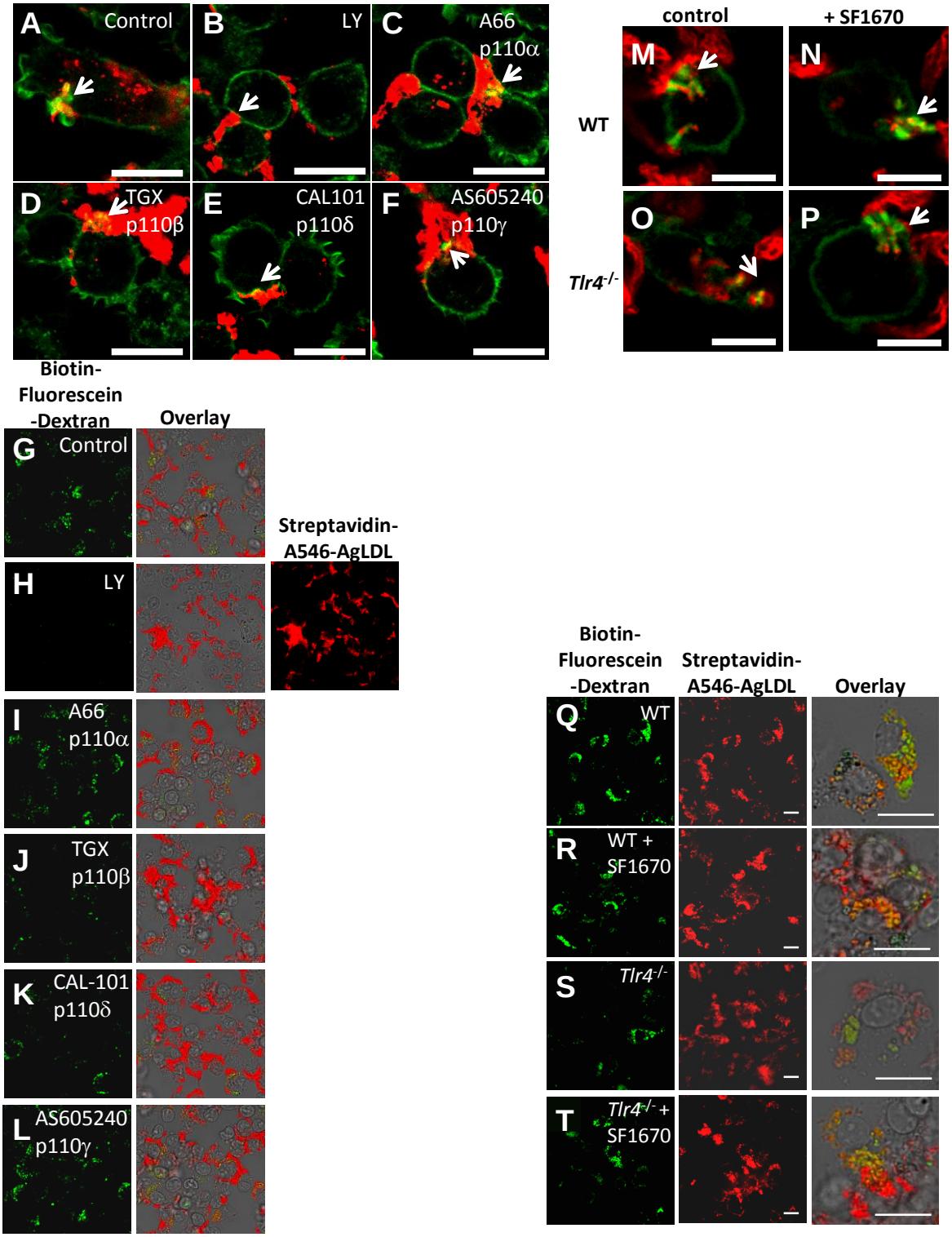

Figure VII. PI3 kinase regulates actin polymerization and lysosome exocytosis to the LS. (A-F) Representative images from Figure 4A showing actin polymerization at the LS in J774 cells pre-treated with DMSO (control), LY294002 (50 μM), p110α inhibitor A66 (8 μM), p110β inhibitor TGX-221 (2 μM), p110δ inhibitor CAL-101 (2 μM) and p110γ inhibitor AS-605240 (2 μM) for 1 hr prior to treatment with A546-agLDL for 1 hr in the presence of inhibitors. (G-L) Representative images from Figure 4B showing lysosome exocytosis at the LS in J774 cells pre-treated with DMSO (control), LY294002 (50 μM), p110α inhibitor A66 (8 μM), p110β inhibitor TGX-221 (2 μM), p110δ inhibitor CAL-101 (2 μM) and p110γ inhibitor AS-605240 (2 μM) for 1 hr prior to treatment with Streptavidin-A546-agLDL for 90 min in the presence of inhibitors. (M-P) Representative images from Figure 4E showing actin polymerization in WT and *Tlr4*$^{-/-}$ BMMs pre-treated with DMSO control or PTEN inhibitor SF1670 (1 μM) for 1 hr prior to treatment with A546-agLDL for 1 hr in the presence of inhibitors. (Q-T) Representative images from Figure 4F showing WT and *Tlr4*$^{-/-}$ BMMs pre-treated with DMSO control or PTEN inhibitor SF1670 (1 μM) for 1 hr prior to treatment with Streptavidin-A546-agLDL for 90 min in the presence of inhibitors. Scale bars 20 μm.

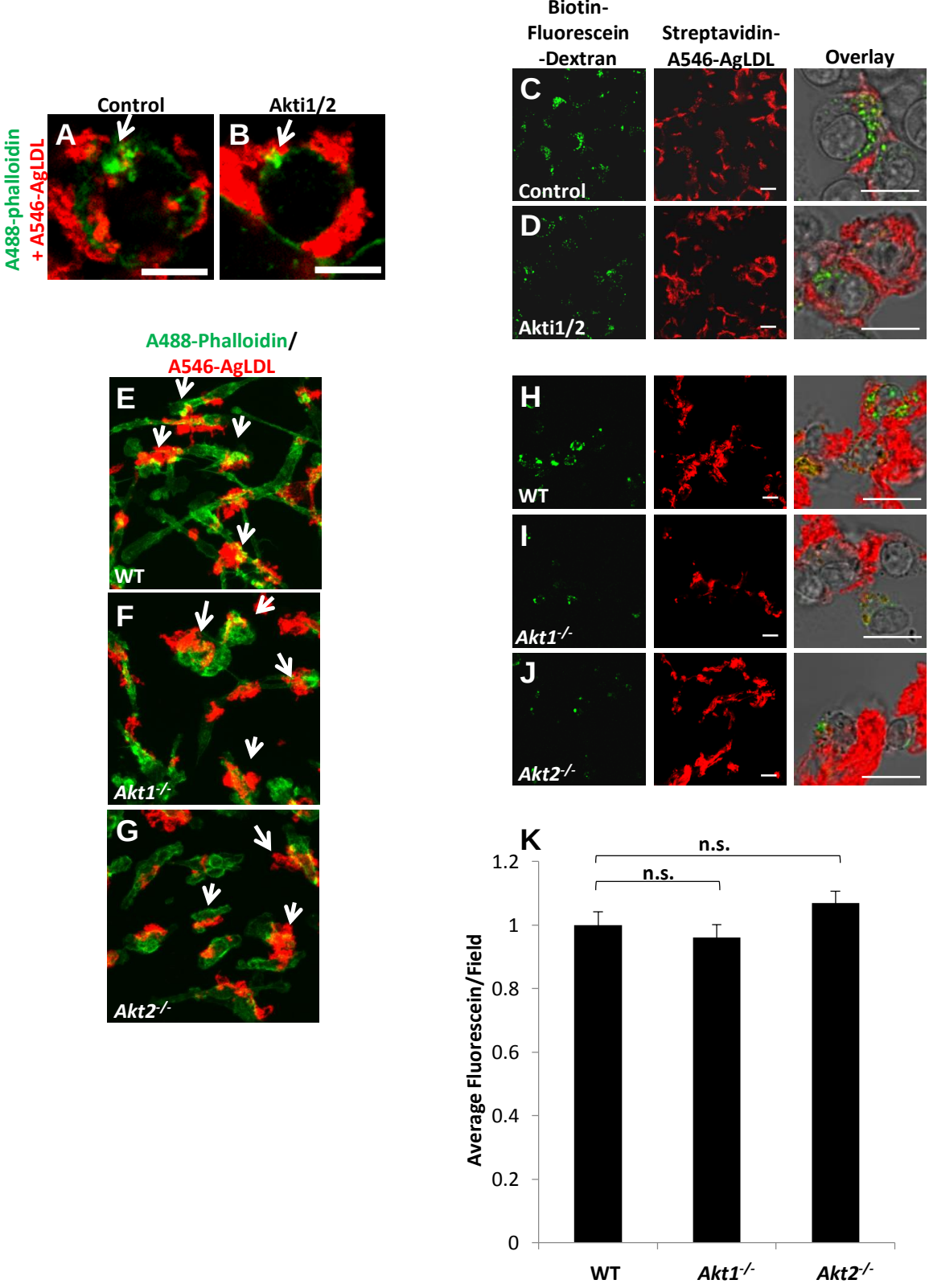

Figure VIII. Akt can promote actin polymerization and lysosome exocytosis in response to agLDL. (A-B) Representative images from Figure 5A showing actin polymerization at the LS in J774 cells pre-treated with DMSO (control) or Akti1/2 for 1 hr prior to treatment with A546-agLDL for 1 hr in the presence of inhibitor. (C-D) Representative images from Figure 5B showing lysosome exocytosis at the LS in J774 cells pre-treated with DMSO (control) or Akti1/2 for 1 hr prior to treatment with Streptavidin-A546-agLDL for 90 min in the presence of inhibitor. (E-G) Representative images from Figure 5C showing actin polymerization at the LS in WT, *Akt1*$^{-/-}$ and *Akt2*$^{-/-}$ BMM treated with A546-agLDL for 1 hr. (H-J) Representative images from Figure 5D showing lysosome exocytosis at the LS in WT, Akt1$^{-/-}$ and Akt2$^{-/-}$ BMM treated with Streptavidin-A546-agLDL for 90 min. (K) WT, *Akt1*$^{-/-}$and *Akt2*$^{-/-}$ BMMs were treated overnight with fluorescein-biotin-dextran and dextran loading in lysosomes was quantified via confocal microscopy Scale bars 20 μm. n.s. is non significant.

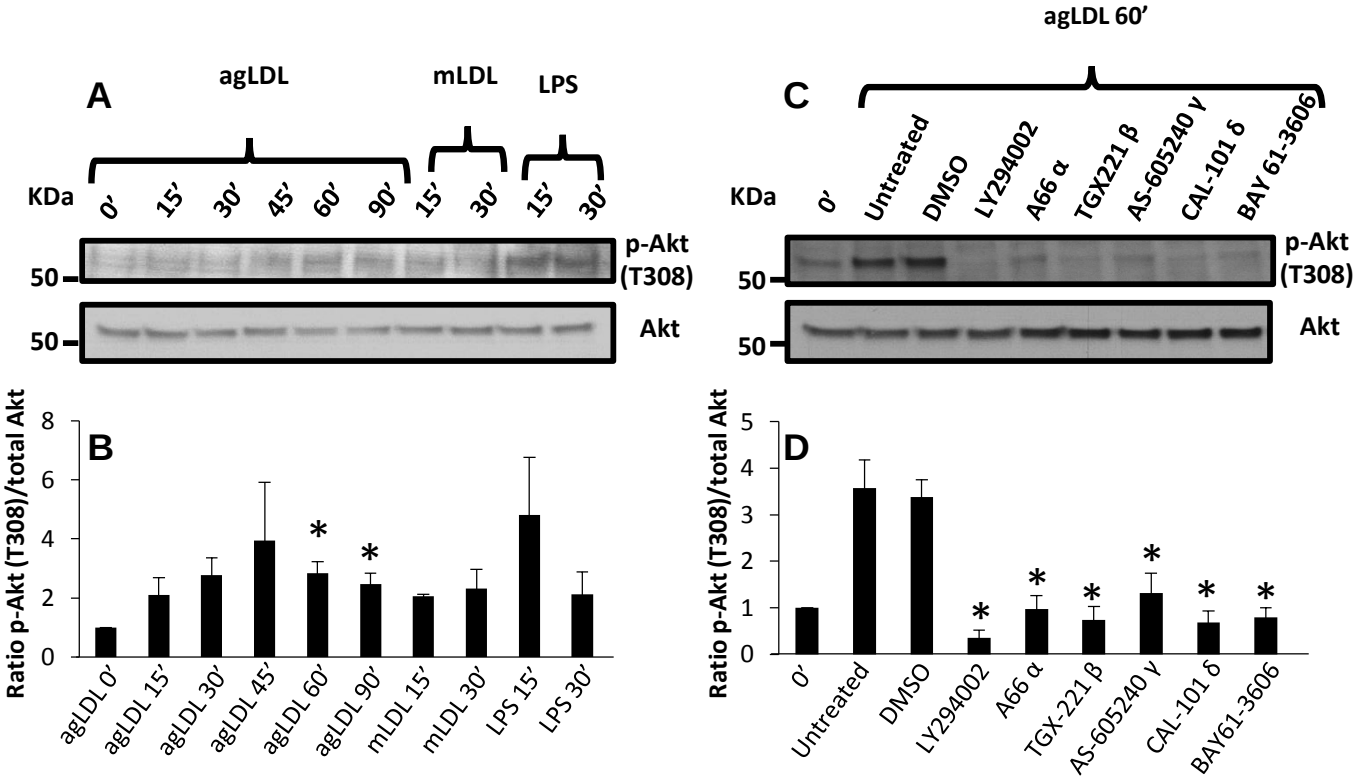

Figure IX. AgLDL-stimulated Akt activation occurs in a PI3K/SYK dependent manner. (A) J774 cells were treated with agLDL (1 mg/mL), mLDL (1 mg/mL) or LPS (100 ng/mL) for indicated periods of time. Ratios of phosphorylated to total protein were obtained by densitometry analysis for (B) Akt (T308). (C) J774 cells were pre-treated for 1 hr with various inhibitors (LY294002 50 μM, A66 8 μM, TGX-221 2 μM, AS-605240 2 μM, CAL-101 2 μM, and BAY 61-3606 5 μM), left untreated or treated with DMSO control, and subsequently incubated with agLDL (1 mg/mL) for 1 hr in the presence of inhibitors. Ratios of phosphorylated to total protein were obtained by densitometry analysis for (D) Akt (T308). Data were compiled from 3 independent experiments. Error bars represent the SEM. * $p < 0.05$.

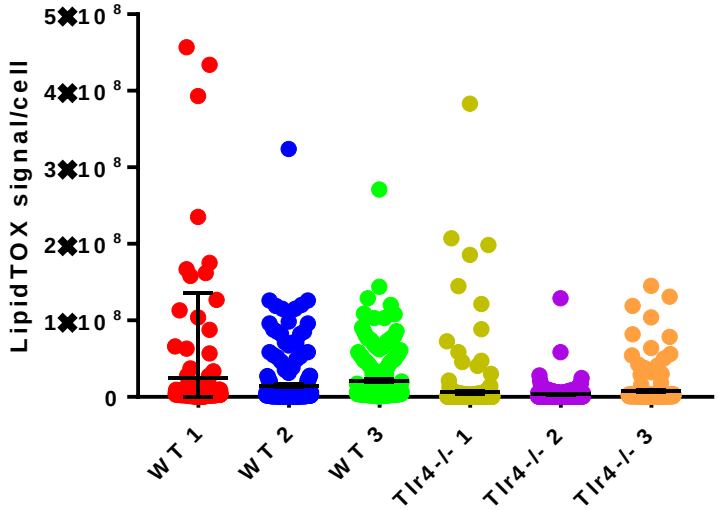

Figure X. Macrophage deficiency of TLR4 protects against cholesterol uptake and foam cell formation *in vivo* during atherosclerosis. *Ldlr*$^{-/-}$ mice were gamma irradiated and reconstituted with WT or *Tlr4*$^{-/-}$ marrows. Mice received a HFD for 16 weeks and were sacrificed. Aortas were digested, and single cell suspensions were centrifuged onto coverslips. Cells were stained to detect neutral lipid (LipidTOX green). Data are split per mouse and correspond to data shown in Figure 7L.

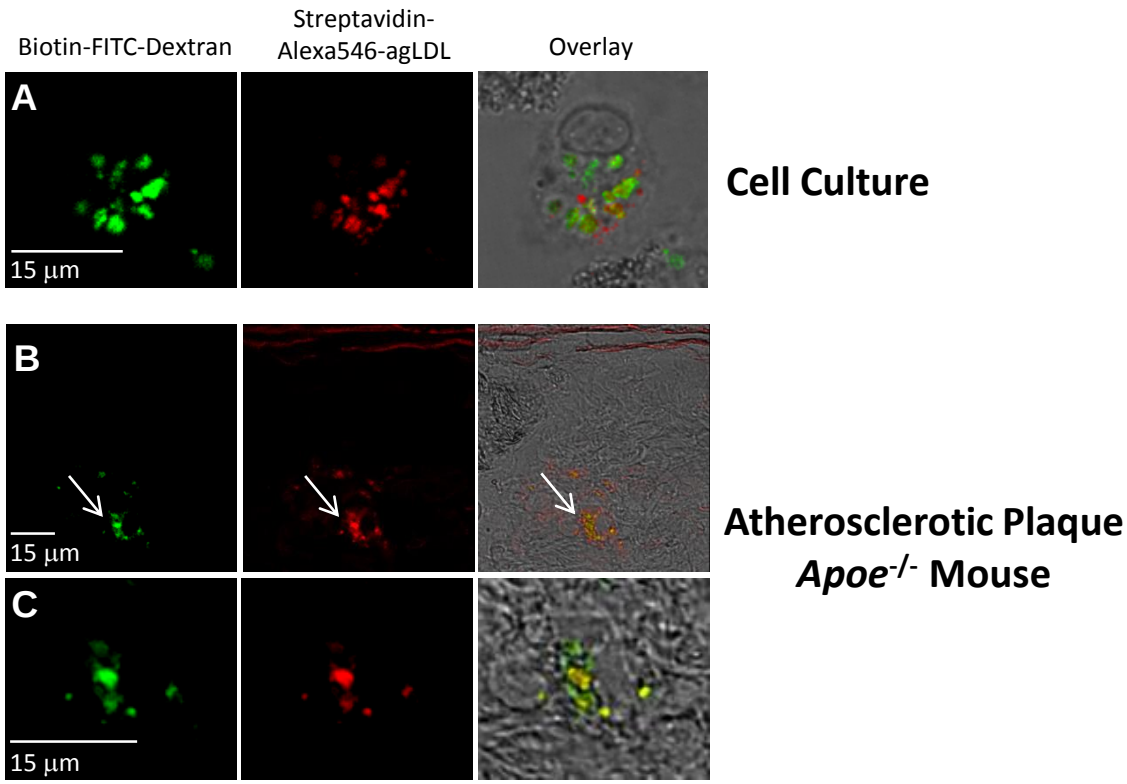

Figure XI. Comparison of LS morphology in vitro and in vivo. (A) J774 cells with their lysosomes loaded with biotin-fluorescein-dextran were incubated with streptavidin-A546-agLDL for 90 min, fixation and permeabilized. (B, C) Apoe$^{-/-}$ mice on a HFD were injected with streptavidin-A546-LDL 1 days prior to injection with BMMs with their lysosomes loaded with biotin-fluorescein-dextran. 3 days after adoptive transfer mice were sacrificed, and the aortas were harvested, sectioned and examined by confocal microscopy.

Major Resources Tables

Animals

Species	Vendor or Source	Background Strain	Sex
Mouse	The Jackson Laboratory	C57BL/6J (stock #000664)	F
Mouse	The Jackson Laboratory	Tlr4-/- (on C57BL/6J background) (stock #007227)	F
Mouse	The Jackson Laboratory	MyD88-/- (on C57BL/6J background) (stock #009088)	F
Mouse	The Jackson Laboratory	Cd14-/- (on C57BL/6J background) (stock #003726)	F
Mouse	The Jackson Laboratory	Trif-/- (on C57BL/6J background) (stock #005037)	F
Mouse	The Jackson Laboratory	Ldlr-/- (on C57BL/6J background) (stock #002207)	F
Mouse	The Jackson Laboratory	Cd36-/- (on C57BL/6J background) (stock #019006)	F
Mouse	The Jackson Laboratory	Scara1-/- (on C57BL/6J background) (stock #006096)	F
Mouse	The Jackson Laboratory	ApoE-/- (on C57BL/6J background) (stock # 002052)	F
Mouse	Dr. Morris Birnbaum (University of Pennsylvania, School of Medicine)	Akt1-/- (on C57BL/6J background)	F
Mouse	Dr. Morris Birnbaum (University of Pennsylvania, School of Medicine)	Akt2-/- (on C57BL/6J background)	F

Antibodies

Target antigen	Vendor or Source	Catalog #	Working concentration	Lot # (preferred but not required)
Phospho-Akt (T308)	Cell Signaling	2965	0.7 µg/mL	
Phospho-Akt (S473)	Cell Signaling	4060	0.09 µg/mL	
Akt (pan)	Cell Signaling	4691	0.035 µg/mL	
SYK	Cell Signaling	2712	0.073 µg/mL	

GAPDH	Abcam	Ab9485	0.4 µg/mL	
CD284(TLR4)/MD-2	BD Biosciences	562221	3.33 µg/mL	
Rat IgD2a, κ isotype control	BD Biosciences	555840	3.33 µg/mL	
F4/80	Abcam	Ab6640	3.33 µg/mL	

Cultured Cells

Name	Vendor or Source	Sex (F, M, or unknown)
J774A.1	ATCC	Female
RAW 264.7	ATCC	Male
J774A.1 shRNA control	Dr. Yuri Miller (University of San Diego)	Female
J774A.1 Tlr4 KD	Dr. Yuri Miller (University of San Diego)	Female